Endocrine Journal 2005, **52** (3), 309–316

Papillary Thyroid Carcinoma without Metastases Manifesting as an Autonomously Functioning Thyroid Nodule

TAKAFUMI MAJIMA*,**, KENTARO DOI*, YASATO KOMATSU**, HIROSHI ITOH**, ATSUSHI FUKAO***, MICHIKA SHIGEMOTO*, CHIEKO TAKAGI*, JERRY CORNERS#, NAOMI MIZUTA##, RYOHEI KATO### AND KAZUWA NAKAO**

**Department of Endocrinology and Metabolism, Rakuwakai Otowa Hospital, Kyoto 607-8062, Japan*
***Department of Medicine and Clinical Science, Kyoto University Graduate School of Medicine, Kyoto 606-8507, Japan*
****Department of Psychosomatic Medicine, Rakuwakai Otowa Hospital, Kyoto 607-8062, Japan*
#Medical Adviser, Rakuwakai Otowa Hospital, Kyoto 607-8062, Japan
##Department of Pathology, Kyoto-Katsura Hospital, Kyoto 615-8256, Japan
###Department of Pathology, Interdisciplinary Graduate School of Medicine and Engineering, University of Yamanashi, Yamanashi 409-3898, Japan

Abstract. A 59-year-old woman with papillary thyroid carcinoma inside of an autonomously functioning thyroid nodule is described in this report. The patient was referred to our clinic because of rapid weight loss and swelling on the left side of the neck. Ultrasonography of the thyroid demonstrated a nonhomogeneous nodule in the lower part of an enlarged left lobe. Both ^{99m}Tc and ^{123}I thyroid scintigraphic imaging showed a hot area corresponding to the nodule with lower uptake in the remaining thyroid tissue. Histopathological examination of the nodule revealed papillary adenocarcinoma, and the immunohistochemistry proved weak but positive staining for triiodothyronine and thyroxine. Based on these findings, the nodule was diagnosed as a functioning papillary adenocarcinoma. Although thyroid carcinoma manifesting as a hot nodule on the radionuclide isotope scan is an extremely rare occurrence, the current case is clinically important because it suggests that the diagnosis of a hot nodule cannot always rule out thyroid carcinoma in the nodule, and that even a hot nodule requires careful management so that the malignancy is not overlooked.

Key words: Papillary thyroid carcinoma, Hyperfunctioning thyroid carcinoma, Hot nodule, Autonomously functioning thyroid nodule, Metastasis

(*Endocrine Journal* **52**: 309–316, 2005)

HYPERTHYROIDISM due to thyroid carcinoma is a rare but well-recognized clinical phenomenon [1, 2]. This situation has been generally described as the result of excessive production of thyroid hormone by extensive metastatic lesions [2–8]. On the other hand, a nonmetastatic hyperfunctioning thyroid carcinoma is extremely rare [1, 2, 9, 10]. Therefore, it is commonly believed that the diagnosis of a solitary autonomously functioning thyroid nodule (AFTN), a solitary "hot" nodule on radionuclide imaging, can almost always rule out malignancy in the nodule [1, 9, 10]. However, in a very few cases, solitary hot nodules do harbor malignancy [1, 2, 9, 10].

In this report, we present a rare case of papillary carcinoma without metastases manifesting as an AFTN.

Received: November 5, 2004
Accepted: February 9, 2005
Corresponding to: Kentaro DOI, M.D., Ph.D., Department of Endocrinology and Metabolism, Rakuwakai Otowa Hospital, 2 Otowa Chinji-cho, Yamashina-ku, Kyoto 607-8062, Japan

Case Report

A 59-year-old Japanese woman was first referred to Otowa Clinic on 3 December 2002 because of rapid loss of weight and an enlarged painless mass on the left side of neck. She had noticed the enlarged neck mass five years earlier, and complained of compressive neck

symptoms, but no dysphagia, hoarseness, or shortness of breath. Despite a good appetite, she lost 7 kg of body weight (from 50 kg to 43 kg) over the past 3 months. Other signs or symptoms of hyperthyroidism were not present. She had neither a family history of thyroid diseases nor a past history of radiation to the head or neck.

On physical examination, her blood pressure and pulse were normal. An enlarged painless mass (approximately 9 cm) with an irregular surface was palpated on the anterior left side of her neck. A nontender and rather hard nodule (approximately 2 cm) was palpable within the lower part of the neck mass. No lymph nodes were palpable in the neck or supraclavicular region. Physical examination was otherwise unremarkable.

Ultrasonography of the thyroid revealed a diffuse enlargement of the left lobe with a mild hypoechoic pattern, and a poorly-demarcated nonhomogeneous nodule with cystic degeneration and calcification, measuring 1.5 cm at the lower end of the left lobe (Fig. 1 A, B). Neck CT scan showed some tracheal deviation to the right without narrowing the airway.

Routine laboratory data showed no abnormality. However, thyroid function tests showed elevated free triiodothyronine (T3) of 4.4 pg/ml (normal; 2.4–4.3 pg/ml) and free thyroxine (T4) of 2.7 ng/dl (normal; 0.8–2.1 ng/dl), and undetectable thyroid-stimulating hormone (TSH) of <0.01 μIU/ml (normal; 0.24–3.70 μIU/ml). Serum thyroglobulin was 520.0 ng/ml (normal; <45 ng/ml). Thyroid stimulating antibody (TSAb), antithyroglobulin (TgAb) and anti-thyroperoxidase (TPOAb) antibodies, and TSH receptor antibody (TRAb) were all negative.

A thyroid technetium-99m (^{99m}Tc) scintigram demonstrated a hot area, with no cold area inside, corresponding to the nodule in the left lower lobe (Fig. 2). Three-hour and 24-hour radioactive iodine thyroid uptakes were 5.00% (normal: 5–15%) and 13.54% (normal: 10–40%), respectively. A thyroid iodine-123 (^{123}I) scintigram also showed a hot area corresponding to the thyroid nodule, with lower uptake in the remaining thyroid tissue (Fig. 3).

Fine needle aspiration biopsy (FNAB) of the nodule was performed. Atypical cells which had large nuclei with a pale ground-glass appearance were found in biopsy specimens from the nodule. The nodule was interpreted as a papillary adenocarcinoma. No malignancy was detected by FNAB of the enlarged left lobe

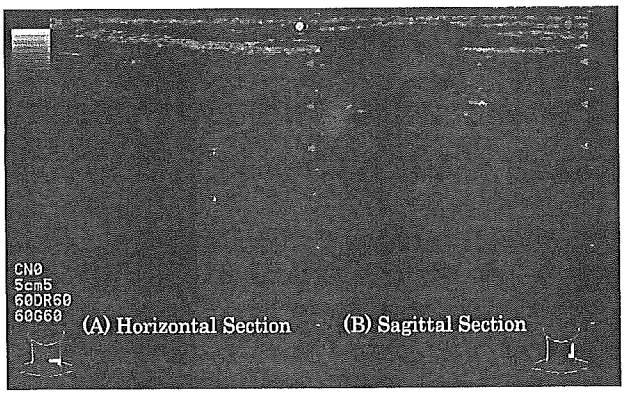

Fig. 1. Ultrasonography of the left thyroid lobe. (A) Horizontal section. (B) Sagittal section.

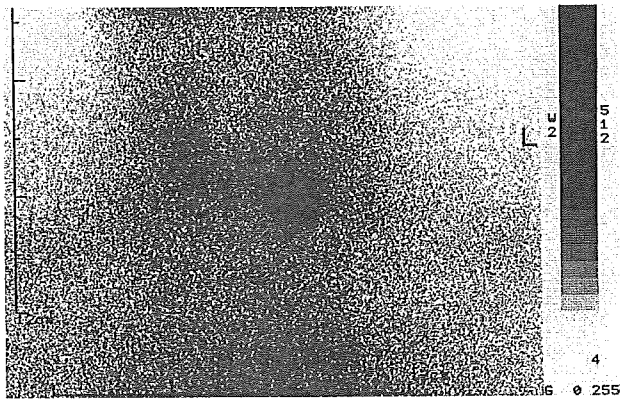

Fig. 2. Thyroid ^{99m}Tc scintigram demonstrating a hot nodule in the left lobe. The rest of the gland shows suppressed activity.

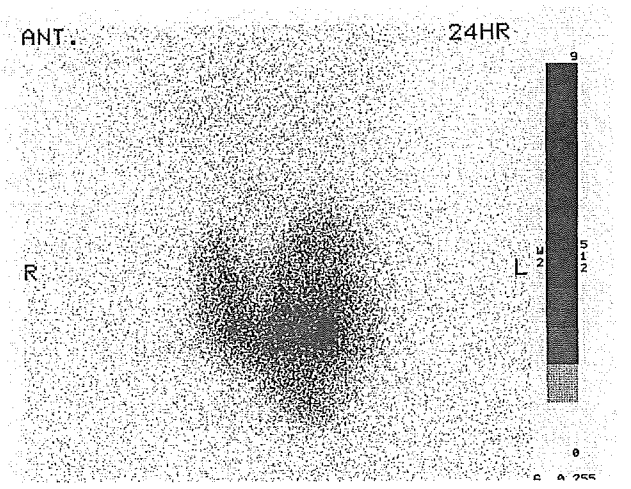

Fig. 3. Thyroid ^{123}I scintigram demonstrating a hot nodule in the left lobe. The rest of the gland shows suppressed activity.

except in the nodule. She received Lugol's solution for 5 days immediately before the operation. A left thyroid lobectomy and isthmectomy were performed on 16th January 2003. At neck exploration, the enlarged left lobe was diffusely elastic and soft, and did not show either adhesion or invasion to the surrounding tissue. The left lobe, the isthmus and the paratracheal lymph nodes were removed, and the left recurrent laryngeal nerve was preserved.

Postoperative histological examination revealed a papillary adenocarcinoma situated within the nodule of the left lower lobe (Fig. 4A). Macroscopically, the nodule was whitish, measuring 1.5 cm in diameter (Fig. 5). It was relatively well circumscribed but not encapsulated, had a granular appearance, and bulged on the thyroid surface (Fig. 5). Microscopically, the

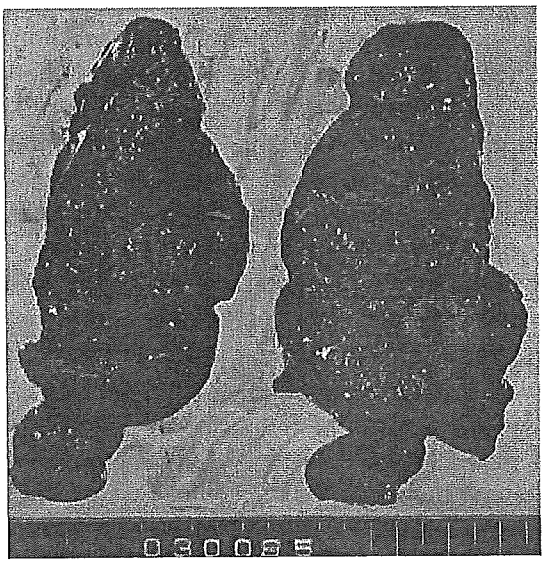

Fig. 5. Cross-section through the left thyroid lobe.

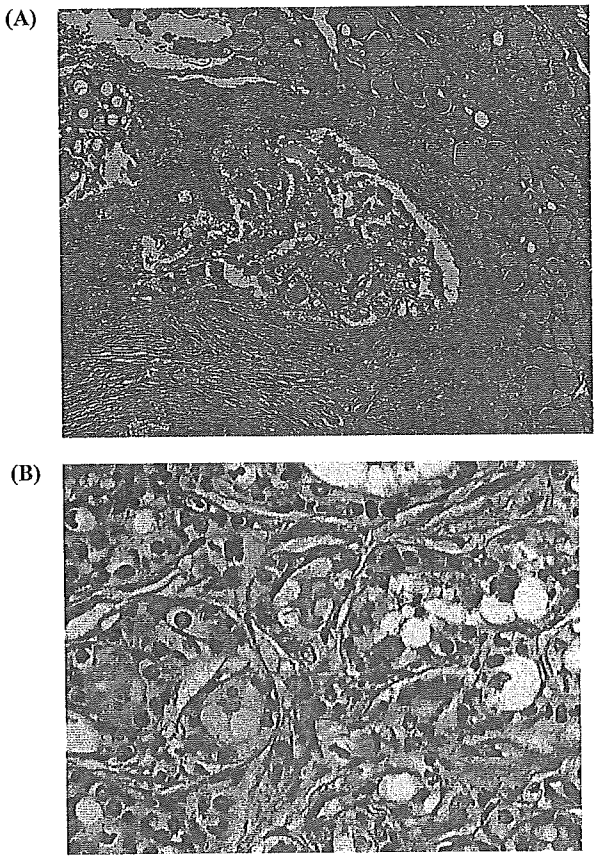

Fig. 4. (A) Histologic appearance of the thyroid tumor demonstrating papillary structures with a follicular pattern (Hematoxylin-eosin stain; × 100). (B) The nuclei of the carcinoma cells showing characteristic nuclear features seen in papillary adenocarcinoma, specifically, ground-glass nuclei, grooves, and pseudoinclusions (Hematoxylin-eosin stain; × 400).

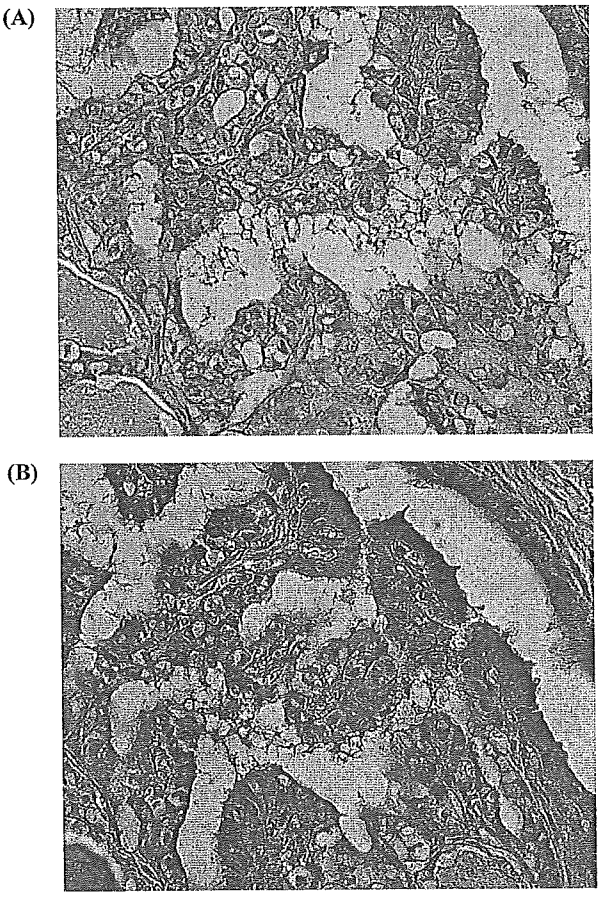

Fig. 6. Immune staining for T3 (A) and T4 (B) showing that the immunohistochemical examination of the neoplastic tissue was weakly but still rather convincingly positive for T3 and T4 (× 200).

nodule contained mainly carcinoma cells but there were also islands of scattered, normal small follicles, interstitial fibrosis, and hyalinization. Malignant growth of carcinoma cells (approximately 1.0 cm) with other multiple small foci of carcinoma cells within the nodule did not infiltrate the tissue outside the nodule, and showed a papillary structure suggestive of papillary carcinoma. The nuclei of the carcinomatous cells had the characteristic nuclear features seen in papillary carcinoma: ground-glass nuclei, grooves, and pseudoinclusions (Fig. 4B). The surrounding thyroid tissue showed a macrofollicular architecture with no evidence of lymphocytic infiltration identified. No histologic evidence of Graves' disease, or Hashimoto's disease, or malignancy was found. The result of immunohistochemical examination of the carcinomatous cells in the nodule was weakly but still definitely positive for T3 and T4 (Fig. 6 A, B). No metastatic foci were recognized in the four resected lymph nodes.

Postoperatively she had mild and transient hypocalcemia which normalized without medication in 1 week. Her TSH has been kept around 0.5 μU/ml with 25 μg of levothyroxine daily. Three months postoperatively, her weight came back to 48 kg. No other complications have occurred in the patient's postoperative course so far.

Discussion

Our patient presented with a palpable thyroid nodule in an enlarged left thyroid lobe and hyperthyroidism with the absence of TSAb, TRAb, TgAb, and TPOAb. Despite undetectable TSH levels, both ^{99m}Tc and ^{123}I thyroid scintigraphic imaging showed a hot nodule corresponding to the nodule, with lower uptake in the remaining thyroid tissue. The nodule was considered to be AFTN, which is a rare condition representing a low percentage of all solitary thyroid nodules (varying from 6% to 20%) [11, 12]. FNAB and postoperative histopathological examination showed the nodule to be a papillary adenocarcinoma, whereas the extranodular tissue of the left thyroid lobe showed a macrofollicular architecture with no evidence of lymphocytic infiltration or malignancy, and was considered a simple goiter, which is defined as noninflammatory, nonneoplastic, diffuse or nodular enlargement of the thyroid gland without causing hyperthyroidism [13, 14].

The major determinant for thyroid growth has long been considered to be the TSH level [13]. However, this is inconsistent with the observation that the serum TSH concentration is normal in most patients with nontoxic goiter [13, 15]. In our case, regression of the goiter was not found regardless of suppressed TSH. Therefore, higher TSH levels as the sole factor responsible for goiter appears to be an oversimplification [13]. Goiter should be regarded as a complex trait in which genetic susceptibility [13, 16], enviromental factors [13], TSH, growth factors [13, 17, 18], and angiogenic substances [13, 19, 20] either play a distinct and separate role or act synergistically through complex interaction mechanisms [13]. However, the relative contributions of these factors to the goitrogenic process have yet to be clarified [13].

It should be noted in our case that the papillary thyroid carcinoma found was as an AFTN. The incidence of thyroid carcinoma in a hot nodule is reported to be low by most authors [1, 2, 9, 10, 21, 24, 25, 27, 28], but is somewhat higher in other retrospective studies (Table 1) [22, 23, 26, 27, 30]. Actually, thyroid carcinoma in a hot nodule has been described in numerous case reports [3–8, 11, 12, 31–46], as well as in ours. However, unlike our case, most of these cases show a cold area within a hot nodule as Tsuboi *et al.* [42] mention in their report, indicating that the thyroid carcinoma itself did not produce thyroid hormone. Hyperfunctioning thyroid carcinoma is thus considered even more infrequent. In addition, hyperfunctioning thyroid carcinoma has been described generally due to extremely extensive functioning metastases [2–8], most

Table 1. Collective experience with thyroid carcinoma in a hot nodule

Author and year		Thyroid carcinoma in the hot nodule		Hot nodule
		the number	the incidence	the number
Ito and Mimura [21]	1983	(4)	(3.9)%	104
Croom *et al.* [22]	1987	2	11.3%	12
Smith *et al.* [23]	1988	2	6.7%	30
Rieger *et al.* [24]	1989	1	0.09%	1108
Ahujya *et al.* [25]	1991	0 (2)	0.0 (0.7)%	298
Mizukami *et al.* [26]	1994	2	11.8%	17
Mann *et al.* [27]	1998	(9)	(1.8)%	760
Chao *et al.* [28]	1999	(1)	(0.4)%	265
Harach *et al.* [29]	2002	6	8.2%	73
Gabriele *et al.* [30]	2003	3	4.7%	64

Parentheses means inclusion of thyroid carcinoma nearby (outside) the hot nodule.

of which have almost always been follicular carcinoma [2, 8]. No less than 50 such cases have been described in the literature, and are well summarized by Paul and Sisson [2]. In their review of 48 cases, distant metastases were present in 83.3% of the patients, with follicular carcinoma in 89.6% of them.

On the other hand, the carcinoma presenting as AFTN in this case was a nonmetastatic hyperfunctioning papillary thyroid carcinoma. Some authors maintain that, in the reported cases of carcinoma presenting as an AFTN, the carcinoma is only incidentally located in a hot nodule [1, 23]. However, in our case, the immunohistochemical study of the carcinoma cells was positive for both hormones T3 and T4. Scintigraphically our case did not have a cold area within the hot nodule, although we cannot rule out the possibility that the carcinoma in our case might have been too small or too localized to exhibit cold lesion. These findings suggest that our case is not a coincidental association of hyperthyroidism and carcinoma but a rare hyperfunctioning papillary thyroid carcinoma.

Rosa *et al.* [12] reviewed 17 cases such as ours in 1990. To our knowledge, there are now 25 cases of nonmetastatic thyroid carcinoma mimicking an AFTN described in the literature (Table 2) [11, 12, 31–46]. Women were far more often affected than men (ratio female/male = 22/3), but there was no significant peak period with regard to age. Interestingly, the histological finding of these tumors was principally papillary carcinoma [12, 31–38, 42, 43, 45, 46], as opposed to that of metastatic functioning carcinomas predominantly being follicular type [2]. This is in agreement with our case.

The reason why these carcinomas were able to produce excessive hormone without extensive metastases may be due to the gene mutations reported to occur in AFTN, including mutations of G protein α chain (Gsα) gene and TSH receptor gene with associated elevated intracellular cAMP [47]. Russo *et al.* [48] reported the first case of an activating mutation of the TSH receptor gene in an autonomously hyperfunctioning thyroid carcinoma. By contrast, Bourasseau *et al.* [49] denied TSH receptor and Gsα gene mutation in hyperfunctioning thyroid carcinoma. Further studies are thus needed to clarify these issues.

Clinically, it is important to predict the incidence of

Table 2. Reported cases of thyroid carcinoma without metastases mimicking an autonomously functioning thyroid nodule

Case No.	Author and year		Age/Gender	Histology of carcinoma	Clinical state
1	Dische S [11]	64'	42/F	follicular	Hyperthyroidism
2	Sussman *et al.* [31]	68'	6/F	papillary	Hyperthyroidism
3	Guinet *et al.* [32]	72'	59/F	papillary	Hyperthyroidism
4			54/F	papillary	Euthyroidism
5	Hopwood *et al.* [33]	76'	16/F	papillary	Euthyroidism
6	Abdel-Razzak and Christie [34]	79'	19/F	papillary	Euthyroidism
7	Baumann *et al.* [35]	79'	64/F	follicular	Hyperthyroidism
8			52/F	follicular	Hyperthyroidism
9			76/F	follicular	Hyperthyroidism
10			86/F	papillary	Hyperthyroidism
11	Nemec *et al.* [36]	82'	22/F	papillary	Hyperthyroidism
12	Sobel *et al.* [37]	85'	27/F	papillary	Hyperthyroidism
13			14/M	papillary	Hyperthyroidism
14			32/F	papillary	Hyperthyroidism
15	Fukata *et al.* [38]	87'	70/F	papillary	Euthyroidism
16	Nagai *et al.* [39]	87'	11/F	follicular	Euthyroidism
17	Tsuchiya *et al.* [40]	87'	66/M	follicular	Euthyroidism
18	Rosa *et al.* [12]	90'	25/F	papillary	Hyperthyroidism
19	Rivas *et al.* [41]	95'	42/F	medullary	Euthyroidism
20	Tsuboi *et al.* [42]	95'	69/M	papillary	Hyperthyroidism
21	Appetecchia and Ducci [43]	98'	23/F	papillary	Hyperthyroidism
22	Schneider *et al.* [44]	00'	44/F	follicular	Euthyroidism
23	Yaturu and Fowler [45]	02'	39/F	papillary	Euthyroidism
24	Hayata *et al.* [46]	03'	51/F	papillary	Hyperthyroidism
25	Present case	04'	59/F	papillary	Hyperthyroidism

malignancy in hot thyroid nodules. The classical benign AFTN often occurs in the 30s or 40s, has a history of long-standing and slowly expanding mass in the neck, and usually presents as a smooth, well-defined, round or ovoid mass that is firm and moves freely [9, 50]. In our case, AFTN occurred at a somewhat older age compared with the classical benign AFTN, but otherwise there were no significant differences. Among patients with classical AFTN, about 20 percent have thyrotoxicosis; these are mostly patients 40 years of age or older with a nodule 2.5 cm or more in diameter [9, 50]. However, in our case, the nodule was smaller in diameter, and the patient was 59 years old. In addition the hyperthyroidism of classical AFTN is generally milder than that of Graves' disease and, as in our case, is notable for the absence of infiltrative orbitopathy and myopathy [50]. Reports in the literature [9] indicate significant difficulty in determining the risk that AFTN will undergo malignant degeneration. However, some clinical findings are reported as the risk factors for malignancy: Age <20 or >60 years, male sex, a family history of medullary or papillary thyroid cancer or of familial adenomatous polyposis (Gardner's syndrome), a past history of head or neck radiation, rapid tumor growth, irregular outline, fixation to adjacent structures, symptoms of tumor invasion, and metastases such as enlarged regional lymph nodes [2, 9, 12, 45]. On the other hand, young women, an excessive production of T3, and conflicting results between ^{99m}Tc and ^{123}I scintigram have been reported as unique risk factors of malignancy in a hot nodule [12, 51].

In actual practice, however, few patients have these symptoms, and most nodules are nearly asymptomatic, as in our case [9, 12]. In the case of metastatic thyroid carcinoma, hot nodules outside the thyroid can be helpful in diagnosis of malignancy. But, especially in the case of nonmetastatic hyperfunctioning thyroid carcinoma, it is somewhat difficult at present to predict the existence of malignancy in the hot nodule. Therefore, FNAB, which is safe, inexpensive, and particularly useful for the diagnosis [9, 12, 28, 37], should be performed in a hot as well as cold thyroid nodule [12, 28, 37].

The clinical course of a non-metastatic hyperfunctioning thyroid carcinoma seems to depend on its histologic features, patient's age, and tumor stage at the time of diagnosis [52], but there is still little information available in the literature [12]. It seems that prognosis of metastatic follicular thyroid carcinoma is not defferent with or without hyperthyroidism [2, 53]. However, the prognosis of non-metastatic hyperfunctioning papillary thyroid carcinoma was not fully described in the literature. Recently, Als *et al.* [54] reported the survival analysis of 19 patients with hyperfunctioning thyroid carcinoma. They showed that five-year survival rates for hyperfunctioning thyroid carcinoma ($n = 19$, 56%) and differentiated thyroid carcinoma ($n = 545$, 94.5%) differed significantly (hazard ratio 4.8, $p = 0.001$), although the difference was attenuated by matching for age, sex, and histopathologic type. But in their study, metastatic carcinoma and nonmetastatic carcinoma were dealt with at the same time, because hyperfunctioning thyroid caricinoma was diagnosed when scintigraphic hot thyroid areas were attributable to the thyroid carcinoma and/or total thyroidectomy failed to induce hypothyroidism. Hence, their report does not present enough information about the prognosis of nonmetastatic hyperfunctioning thyroid carcinoma, which we have discussed in this paper.

In conclusion, our case is pathophysiologically interesting when we consider that a papillary thyroid carcinoma could produce hyperthyroidism without metastases, and clinically it is important in suggesting that malignancy cannot always be excluded even in a hot thyroid nodule, and that all thyroid nodules, whether cold or hot, require careful management so that malignancy is not overlooked.

References

1. Rieger R, Pimpl W, Money S, Rettenbacher L, Galvan G (1989) Hyperthyroidism and concurrent thyroid malignancies. *Surgery* 106: 6–10.
2. Paul SJ, Sisson JC (1990) Thyrotoxicosis caused by thyroid cancer. *Endocrinol Metab Clin North Am* 19: 593–612.
3. Girelli ME, Easara D, Rubelo D, Pelizzo MR, Busnardo B, Ziliotto D (1990) Severe hyperthyroidism due to metastatic papillary thyroid carcinoma with favorable outcome. *J Endocrinol Invest* 13: 333–337.
4. Kasagi K, Takeuchi R, Miyamoto S, Misaki T, Inoue D, Shimazu A, Mori T, Konishi J (1994) Metastatic thyroid cancer presenting as thyrotoxicosis: report of three cases. *Clin Endocrinol (Oxf)* 40: 429–434.

5. Yoshimura Noh J, Mimura T, Kawano M, Hamada N, Ito K (1997) Appearance of TSH receptor antibody and hyperthyroidism associated with metastatic thyroid cancer after total thyroidectomy. *Endocr J* 44: 855–859.
6. Suzuki K, Nakagawa O, Aizawa Y (2001) A case of pulmonary metastatic thyroid cancer complicated with Graves' disease. *Endocr J* 48: 175–179.
7. Ishihara T, Ikekubo K, Shimodahira M, Iwakura T, Kobayashi M, Hino M, Oobayashi M, Kohno K, Kimura K, Kawamura S, Kurahachi H (2002) A case of TSH receptor antibody-positive hyperthyroidism with functioning metastases of thyroid carcinoma. *Endocr J* 49: 241–245.
8. Basaria S, Salvatori R (2002) Thyrotoxicosis due to metastatic papillary thyroid cancer in a patient with Graves' disease. *J Endocrinol Invest* 25: 639–642.
9. Mazzaferri EL (1993) Management of a solitary thyroid nodule. *N Eng J Med* 328: 553–559.
10. Mazzaferri EL (1990) Thyroid cancer and Graves' disease. *J Clin Endocrinol Metab* 70: 826–829.
11. Dische S (1964) The radioisotope scan applied to the detection of carcinoma in thyroid swellings. *Cancer* 17: 473–479.
12. De Rosa G, Testa A, Maurizi M, Satta MA, Aimoni C, Artuso A, Silvestri E, Rufini V, Troncone L (1990) Thyroid carcinoma mimicking a toxic adenoma. *Eur J Nucl Med* 17: 179–184.
13. Schlumberger MJ, Filetti S, Hay ID (2003) Nontoxic goiter and thyroid neoplasia. In: Larsen PR, Kronenberg HM, Melmed S, Polonsky KS (eds) Williams of Textbook of Endocrinology 10th edition. Saunders, Philadelphia, 457–490.
14. Murray D (1991) The thyroid gland. In: Kovacs K, Asa S (eds) Functional Endocrine Pathology. Blackwell Scientific Publications, Boston, 293–374.
15. Vassart G, Dumont JE (1992) The thyrotropin receptor and the regulation of thyrocyte function and growth. *Endocr Rev* 13: 596–611.
16. Brix TH, Kyvik KO, Hegedus L (1999) Major role of genes in the etiology of simple goiter in females: a population-based twin study. *J Clin Endocrinol Metab* 84: 3071–3075.
17. Tansey WP, Schaufele F, Heslewood M, Handford C, Reudelhuber TL, Catanzaro DF (1993) Distance-dependent interactions between basal, cyclic AMP, and thyroid hormone response elements in the rat growth hormone promoter. *J Biol Chem* 268: 14906–14911.
18. Wuster C, Steger G, Schmelzle A, Gottswinter J, Minne HW, Ziegler R (1991) Increased incidence of euthyroid and hyperthyroid goiters independently of thyrotropin in patients with acromegaly. *Horm Metab Res* 23: 131–134.
19. Wollman SH, Herveg JP, Zeligs JD, Ericson LE (1978) Blood capillary enlargement during the development of thyroid hyperplasia in the rat. *Endocrinology* 103: 2306–2314.
20. Ramsden JD (2000) Angiogenesis in the thyroid gland. *J Endocrinol* 166: 475–480.
21. Ito K, Mimura T (1983) Autonomously functioning thyroid nodule and its diagnostic problems. *Nippon Rinsho* 41: 1197–1202 (in Japanese).
22. Croom RD 3rd, Thomas CG Jr, Reddick RL, Tawil MT (1987) Autonomously functioning thyroid nodules in childhood and adolescence. *Surgery* 102: 1101–1108.
23. Smith M, McHenry C, Jarosz H, Lawrence AM, Paloyan E (1988) Carcinoma of the thyroid in patients with autonomous nodules. *Am Surg* 54: 448–449.
24. Rieger R, Pimpl W, Money S, Rettenbacher L, Galvan G (1989) Hyperthyroidism and concurrent thyroid malignancies. *Surgery* 106: 6–10.
25. Ahuja S Ahuja S, Ernst H (1991) Hyperthyroidism and thyroid carcinoma. *Acta Endocrinol (Copenh)* 124: 146–151.
26. Mizukami Y, Michigishi T, Nonomura A, Yokoyama K, Noguchi M, Hashimoto T, Nakamura S, Ishizaki T (1994) Autonomously functioning (hot) nodule of the thyroid gland. A clinical and histopathologic study of 17 cases. *Am J Clin Pathol* 101: 29–35.
27. Mann K (1998) Evaluation of risk in autonomously functioning thyroid nodules. *Exp Clin Endocrinol Diabetes* 106 (Suppl 4): S23–S26.
28. Chao TC, Lin JD, Jeng LB, Chen MF (1999) Thyroid cancer with concurrent hyperthyroidism. *Arch Surg* 134: 130–134.
29. Harach HR, Sanchez SS, Williams ED (2002) Pathology of the autonomously functioning (hot) thyroid nodule. *Ann Diagn Pathol* 6: 10–19.
30. Gabriele R, Letizia C, Borghese M, De Toma G, Celi M, Izzo L, Cavallaro A (2003) Thyroid cancer in patients with hyperthyroidism. *Horm Res* 60: 79–83.
31. Sussman L, Librik L, Clayton GW (1968) Hyperthyroidism attributable to a hyperfunctioning thyroid carcinoma. *J Pediatr* 72: 208–213.
32. Guinet P, Tourniaire J, Radi A, Briere J, Bryon PA, Dutrieux N, Guillaud M, Maillet P, Sassolas G, Soustelle J (1972) Hyperthyroidism and thyroid cancer. *Endocrinol Clin* 13: 199–227 (in French).
33. Hopwood NJ, Carroll RG, Kenny FM, Foley TP Jr (1976) Functioning thyroid masses in childhood and adolescence. Clinical, surgical, and pathologic correlations. *J Pediatr* 89: 710–718.
34. Abdel-Razzak M, Christie JH (1979) Thyroid carcinoma in an autonomously functioning nodule. *J Nucl Med* 20: 1001–1002.
35. Baumann K, Weitzel M, Burgi H (1979) Hormone-producing thyroid carcinoma with hyperthyroidism. Analysis of 6 cases and review of the literature. *Schweiz Med Wochenschr* 109: 309–314 (in German).
36. Nemec J, Zamrazil V, Vana S, Pohunkova D, Zeman

V, Nahodil V, Rohling S, Bednar J (1982) Clinical and pathogenetic problems in hyperthyroid syndrome in thyroid cancer. *Acta Univ Carol* (Praha) 28: 119–167.
37. Sobel RJ, Liel Y, Goldstein J (1985) Papillary carcinoma and the solitary autonomously functioning nodule of the thyroid. *Isr J Med Sci* 21: 878–882.
38. Fukata S, Tamai H, Matsubayashi S, Nagai K, Hirota Y, Matsuzuka F, Katayama S, Kuma K, Nagataki S (1987) Thyroid carcinoma and hot nodule. *Eur J Nucl Med* 13: 313–314.
39. Nagai GR, Pitts WC, Basso L, Cisco JA, McDougall IR (1987) Scintigraphic hot nodules and thyroid carcinoma. *Clin Nucl Med* 12: 123–127.
40. Tsuchiya A, Nemoto T, Nomizu S, Satou H, Watanabe I, Abe R (1987) Follicular adenocarcinoma in an autonomously functioning thyroid nodule. *Gan no Rinsho* 33: 65–69 (in Japanese).
41. Rivas I, Gutierrez C, Vendrell J, Razkin S, Richart C (1995) Medullary thyroid carcinoma mimicking an autonomous functioning nodule. *J Endocrinol Invest* 18: 224–227.
42. Tsuboi M, Shigemasa C, Ueta Y, Yoshida A, Kobayashi K, Mori T, Mashiba H (1995) A patient with an autonomously functioning thyroid nodule with papillary adenocarcinoma associated with Graves' hyperthyroidism. *Clin Nucl Med* 20: 985–988.
43. Appetecchia M, Ducci M (1998) Hyperfunctioning differentiated thyroid carcinoma. *J Endocrinol Invest* 21: 189–192.
44. Schneider PW, Meier DA, Balon H (2000) A clear cell variant of follicular carcinoma presenting as an autonomously functioning thyroid nodule. *Thyroid* 10: 269–273.
45. Yaturu S, Fowler MR (2002) Differentiated thyroid carcinoma with functional autonomy. *Endocr Pract* 8: 36–39.
46. Hayata M, Kamei T, Okayasu N, Yoshida M, Banba N, Hattori Y, Kasai K (2003) Functional papillary carcinoma of the thyroid occurred in the Graves' disease. *Clin Endocrinol (Tokyo)* 51: 66–69 (in Japanese).
47. Paschke R, Tonacchera M, Van Sande J, Parma J, Vassart G (1994) Identification and functional characterization of two new somatic mutations causing constitutive activation of the thyrotropin receptor in hyperfunctioning autonomous adenomas of the thyroid. *J Clin Endocrinol Metab* 79: 1785–1789.
48. Russo D, Tumino S, Arturi F, Vigneri P, Grasso G, Pontecorvi A, Filetti S, Belfiore A (1997) Detection of an activating mutation of the thyrotropin receptor in a case of an autonomously hyperfunctioning thyroid insular carcinoma. *J Clin Endocrinol Metab* 82: 735–738.
49. Bourasseau I, Savagner F, Rodien P, Duquenne M, Reynier P, Guyetant S, Bigorgne JC, Malthiery Y, Rohmer V (2000) No evidence of thyrotropin receptor and G(s alpha) gene mutation in high iodine uptake thyroid carcinoma. *Thyroid* 10: 761–765.
50. Davis TF, Larsen PR (2003) Thyrotoxicosis. In: Larsen PR, Kronenberg HM, Melmed S, Polonsky KS (eds) Williams of Textbook of Endocrinology 10th edition. Saunders, Philadelphia, 374–421.
51. dell'Erba L, Gerundini P, Caputo M, Bagnasco M (2003) Association of hyperfunctioning thyroid adenoma with thyroid cancer presenting as "trapping only" nodule at 99mTcO4- scintigraphy. *J Endocrinol Invest* 26: 1124–1127.
52. Mazzaferri EL (1991) Carcinoma of follicular epithelium: radioiodine and other treatment and outcomes. In: Braverman LE, Utiger RD (eds) Werner and Ingbar's the Thyroid: A Fundamental and Clinical Test, 6th edition. Lippincott, Philadelphia, 1138–1165.
53. Lin JD, Chao TC, Hsueh C (2004) Follicular thyroid carcinomas with lung metastases: a 23-year retrospective study. *Endocr J* 51: 219–225.
54. Als C, Gedeon P, Rosler H, Minder C, Netzer P, Laissue JA (2002) Survival analysis of 19 patients with toxic thyroid carcinoma. *J Clin Endocrinol Metab* 87: 4122–4127.

Hypertension
JOURNAL OF THE AMERICAN HEART ASSOCIATION

Role of Natriuretic Peptide Receptor Guanylyl Cyclase-A in Myocardial Infarction Evaluated Using Genetically Engineered Mice

Michio Nakanishi, Yoshihiko Saito, Ichiro Kishimoto, Masaki Harada, Koichiro Kuwahara, Nobuki Takahashi, Rika Kawakami, Yasuaki Nakagawa, Keiji Tanimoto, Shinji Yasuno, Satoru Usami, Yuhao Li, Yuichiro Adachi, Akiyoshi Fukamizu, David L. Garbers and Kazuwa Nakao

Hypertension 2005;46;441-447; originally published online Jul 5, 2005;
DOI: 10.1161/01.HYP.0000173420.31354.ef
Hypertension is published by the American Heart Association. 7272 Greenville Avenue, Dallas, TX 72514
 Print ISSN: 0194-911X. Online ISSN: 1524-4563

Role of Natriuretic Peptide Receptor Guanylyl Cyclase-A in Myocardial Infarction Evaluated Using Genetically Engineered Mice

Michio Nakanishi, Yoshihiko Saito, Ichiro Kishimoto, Masaki Harada, Koichiro Kuwahara, Nobuki Takahashi, Rika Kawakami, Yasuaki Nakagawa, Keiji Tanimoto, Shinji Yasuno, Satoru Usami, Yuhao Li, Yuichiro Adachi, Akiyoshi Fukamizu, David L. Garbers, Kazuwa Nakao

Abstract—Although plasma levels of atrial natriuretic peptide (ANP) and brain natriuretic peptide (BNP) are elevated early after myocardial infarction (MI), the significance is not fully understood. We therefore investigated the function of natriuretic peptides after induction of MI in knockout (KO) mice lacking the natriuretic peptide receptor guanylyl cyclase-A, the receptor for ANP and BNP. KO and wild-type (WT) mice were subjected to left coronary artery ligation and then followed up for 4 weeks. Irrespective of genotype, almost all deaths occurred within 1 week after induction of MI. KO mice showed significantly higher mortality because of a higher incidence of acute heart failure, which was associated with diminished water and sodium excretion and with higher cardiac levels of mRNAs encoding ANP, BNP, transforming growth factor-β1, and type I collagen. By 4 weeks after infarction, left ventricular remodeling, including myocardial hypertrophy and fibrosis, and impairment of left ventricular systolic function were significantly more severe in KO than WT mice. Notably, the enhanced myocardial fibrosis seen in KO mice was virtually absent in infarcted double-KO mice, lacking guanylyl cyclase-A and angiotensin II type 1a receptors, although there was no improvement in survival and no attenuation of cardiac hypertrophy. Thus, guanylyl cyclase-A activation by endogenous cardiac natriuretic peptides protects against acute heart failure and attenuates chronic cardiac remodeling after MI. These beneficial effects are mediated partly through inhibition of the renin-angiotensin system (RAS), although RAS-independent protective actions of guanylyl cyclase-A are also suggested. (***Hypertension.* 2005;46:441-447.**)

Key Words: receptors, angiotensin ■ coronary artery disease ■ hypertrophy ■ remodeling

Early reperfusion therapy and other recent advances in the treatment of acute myocardial infarction (MI) have substantially reduced mortality and cardiovascular morbidity among MI patients. However, the fact that acute heart failure and chronic left ventricular (LV) remodeling continue to be major determinants of clinical outcome after MI highlights the need for a better understanding of the pathophysiological mechanisms involved in those processes. In that regard, accumulating clinical and experimental evidence indicates that inhibition of the renin-angiotensin system (RAS) and the sympathetic nervous system improves postinfarct survival and mitigates LV remodeling and dysfunction.[1–4]

Atrial natriuretic peptide (ANP) and brain natriuretic peptide (BNP) are produced mainly in the atrial and ventricular myocardium, respectively, in response to volume expansion and pressure overload and counteract the effects of the sympathetic nervous system and RAS by promoting diuresis, natriuresis, and vasodilatation. The actions of both peptides are mediated via the natriuretic peptide receptor guanylyl cyclase-A (GC-A), which is expressed in a variety of tissues, including kidneys, blood vessels, adrenal glands, and heart.[5] Plasma levels of natriuretic peptides are elevated in congestive heart failure (CHF) and are frequently used to aid diagnosis of CHF, to assess prognosis, and to tailor therapy.[6–9] In addition, exogenous administration of recombinant natriuretic peptides is now being used therapeutically to treat decompensated CHF.[10]

Plasma natriuretic peptide levels are also elevated early after MI;[11] in particular, the level of BNP has been shown to be a good predictor of LV systolic function and a prognostic indicator of long-term survival.[12] Although in a previous study, we suggested a role for GC-A in myocardial reperfusion injury and inflammation after ischemia-reperfusion,[13] it remains unclear whether activation of the GC-A pathway by endogenous natriuretic peptides has a significant effect on survival or LV remodeling after MI. Therefore, to better

Received November 21, 2004; first decision December 9, 2004; revision accepted April 2, 2005.

From the Department of Medicine and Clinical Science, Kyoto University Graduate School of Medicine (M.N., I.K., M.H., K.K., N.T., R.K., Y.N., K.T., S.Y., S.U., Y.L., Y.A., K.N.), Japan; the First Department of Internal Medicine, Nara Medical University, Japan (Y.S.); the Center for Tsukuba Advanced Research Alliance, Institute of Applied Biochemistry, University of Tsukuba, Ibaraki, Japan (A.F.); and the Howard Hughes Medical Institute and Department of Pharmacology, University of Texas, Southwestern Medical Center at Dallas (D.L.G.).

Correspondence to Ichiro Kishimoto, MD, PhD, Department of Biochemistry, National Cardiovascular Center, Research Institute, 5-7-1 Fujishiro-dai, Suita City, Osaka 565-8565, Japan. E-mail kishimot@ri.ncvc.go.jp

Hypertension is available at http://www.hypertensionaha.org DOI: 10.1161/01.HYP.0000173420.31354.ef

understand the function and significance of the increased natriuretic peptide levels seen after MI, we induced MI by occluding the left coronary artery (LCA) in GC-A knockout (KO) mice and their wild-type (WT) littermates and examined survival, LV structure, LV function, and cardiac gene expression.

Materials and Methods

Experimental Model

All experimental procedures were performed according to Kyoto University standards for animal care. Homozygous GC-A KO mice and their WT littermates were produced from crossing heterozygous mice as described previously,[14] after which male mice were used for experimentation at 8 to 10 weeks of age.

Experimental MI

MI was produced by permanent ligation of the LCA, and sham-operated mice underwent the same operation except for the LCA ligation. Infarct size was calculated and expressed as the ratio of the infarcted circumference divided by total LV circumference, as described previously.[15]

Noninvasive Blood Pressure Measurements

Blood pressures and pulse rates were measured noninvasively in conscious mice using a computerized tail-cuff method (Softron Co, Ltd).

Urine Volume and Sodium Excretion

Animals were kept in individual metabolic cages from the day before surgery until 4 days after surgery. Urine was collected daily, and urine volume and sodium excretion were measured. Data were normalized to body weight (BW).

Cardiac Gene Expression

On day 3 after surgery, hearts were excised and the LVs were snap-frozen in liquid nitrogen. Total RNA was extracted from LVs, and expression of mRNAs was evaluated using quantitative RT-PCR analysis with gene-specific primers and probes in an ABI PRISM 7700 Sequence Detector (Applied Biosystems). Expression of the RNA in question was normalized to that of the corresponding GAPDH mRNA.

Echocardiography Examination

After anesthetizing mice by intraperitoneal administration of a mixture of ketamine (100 mg/kg) and xylazine (5 mg/kg), LV end-diastolic diameter (LVEDD), LV end-systolic diameter (LVESD), percent fractional shortening (%FS), and LV posterior wall (PW) thickness were calculated before (baseline) and 4 weeks after induction of MI using an echocardiographic system (Toshiba Power Vision 8000) equipped with a 12-MHz imaging transducer.

Histological Analysis

To determine the degree of collagen fiber accumulation, we randomly selected 20 fields in 3 separate sections of formalin-fixed ventricles and calculated the ratio of the van Gieson–stained fibrotic area to the total myocardial area using image analysis software (KS400 image system; Zeiss).

Double-KO Mice Lacking GC-A and Angiotensin II Type 1a Receptors

Double-KO (DKO) mice lacking GC-A and angiotensin II type 1a (AT1a) receptors were generated from heterozygous mice after crossing of a single GC-A KO mouse and an AT1a KO mice.[16]

TABLE 1. Baseline Characteristics and Causes of Death After MI

Variables	WT (n=37)	GC-A KO (n=33)
Baseline characteristics		
Age (weeks)	9.6±0.2	9.2±0.1
BW (g)	25.3±0.4	25.7±0.5
Systolic BP (mm Hg)	98.9±1.5	128.3±1.5*
PR (bpm)	569.9±13.9	553.6±10.4
Causes of death, n (%)		
Heart failure	2 (5.4%)	18 (54.5%)*
LV rupture	8 (21.6%)	5 (15.2%)
Unknown	1 (2.7%)	1 (3.0%)

BP indicates blood pressure; PR, pulse rate.
Values are mean±SEM; *$P<0.05$ vs WT mice.

Hydralazine Administration

The blood pressures of GC-A KO mice were reduced to a level comparable to those seen in WT mice by orally administering hydralazine (50 mg/L of drinking water). Hydralazine was started 1 week before MI and continued until death, 4 weeks after MI.

Statistical Analysis

All data are expressed as means±SEM. Analysis of survival after MI was performed using the Kaplan–Meier method with the log-rank test. Data were analyzed by 1-factor ANOVA. If a statistically significant effect was found, a post hoc Newman–Keuls test was performed to isolate the differences between groups. Values of $P<0.05$ were considered significant.

Results

Survival After MI

The baseline characteristics of the KO and WT genotypes are shown in Table 1. There were no differences with respect to age, BW, or pulse rate between the 2 groups, although blood pressure was significantly higher in KO mice, as reported previously.[14,17] Postoperative survival was monitored for 4 weeks (Figure 1). Irrespective of genotype, all deaths but 1 occurred within 1 week after induction of MI; 1 WT mouse

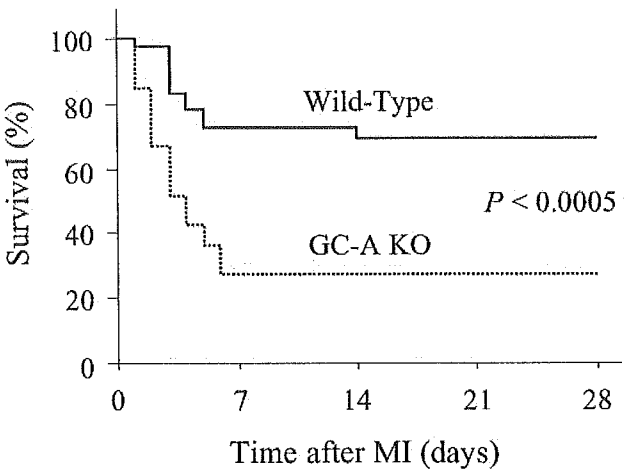

Figure 1. Kaplan–Meier analysis of survival after MI among WT (n=37) and GC-A KO mice (n=33). GC-A KO mice showed a significantly higher 4-week mortality rate than WT mice ($P<0.0005$).

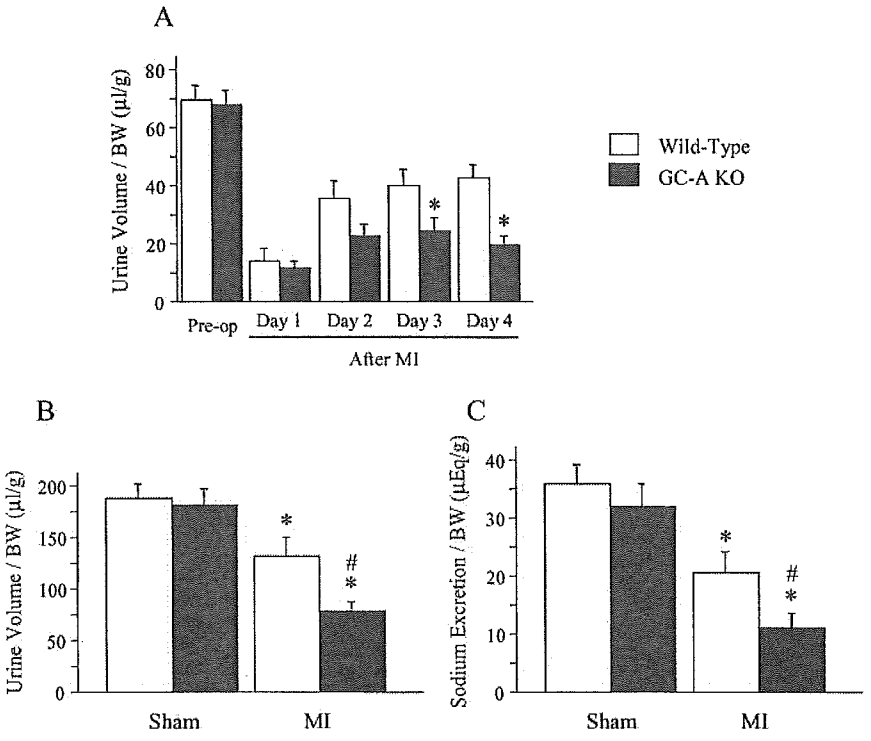

Figure 2. Diuretic and natriuretic responses before and after MI. A, Urine volumes were measured 1 day before (pre-op) and on days 1 through 4 after induction of MI and normalized to the corresponding BWs; *$P<0.05$ vs WT mice on each day. B and C, Total 4-day urine volume (B) and sodium excretion (C) were measured after induction of MI or sham operation and normalized to the corresponding BW. Values are means±SEM (n=12 for WT mice; n=16 for KO mice); *$P<0.01$ vs sham in each strain; #$P<0.05$ vs WT mice with MI.

died on day 14 after MI. Despite the fact that infarct sizes were similar in the 2 groups (KO 43.7±1.2% versus WT 46.8±1.8%), the survival rate was significantly ($P<0.0005$) lower among KO mice (27.3%; 9 of 33) than among WT mice (70.3%; 26 of 37).

Causes of Death

Based on postmortem findings, the causes of death were classified into 3 groups: heart failure, LV rupture, or unknown causes (Table 1). Heart failure was diagnosed from pulmonary congestion with increased lung weight, and LV rupture from the large amount of blood observed filling the chest cavity. The incidence of heart failure was significantly higher among KO mice than WT mice, although there were no significant differences between the 2 groups in the incidences of LV rupture or death by unknown causes.

Natriuretic and Diuretic Responses During Early Phase After MI

As shown in Figure 2A, there was no difference in urine volume between the 2 genotypes before surgery, and urine volume was markedly lower in both groups on day 1 after MI. Thereafter, volume increased gradually in both genotypes, but less so in KO mice. As a consequence, KO mice were producing significantly less urine than WT mice on days 3 and 4 after MI.

When we compared the renal responses of infarcted and sham-operated mice (Figure 2B and 2C), we found that the total 4-day urine volume and sodium excretion after the sham operation were similar for both genotypes. In contrast, over the course of 4 days after induction of MI, KO mice produced significantly less urine and excreted significantly less sodium than WT mice.

Cardiac Gene Expression During Early Phase After MI

On day 3 after sham operation, ventricular levels of ANP and BNP mRNA (Figure 3A and 3B) were higher in KO than WT hearts, probably because of basal LV hypertrophy in the former. In response to MI, both genotypes showed significant upregulation of ANP and BNP mRNA, but the postinfarction levels were still significantly higher in KO mice.

The cardiac expression of the mRNAs for transforming growth factor-β1 (TGF-β1) and type I collagen (Figure 3C and 3D) were similar in sham-operated WT and KO mice. Three days after MI, both genotypes showed significantly upregulated expression of TGF-β1 and type I collagen mRNA, but the postinfarction levels were significantly higher in KO than WT mice.

Echocardiographic Findings During Late Phase After MI

To evaluate chronic LV remodeling, echocardiographic examination of the infarcted mice was performed before (baseline) and 4 weeks after induction of MI (Table 2). Baseline measurements showed KO mice to have greater LVEDD, LVESD, and PW thickness than WT mice, but %FS was similar, as reported previously.[17] Four weeks after MI, both genotypes showed significant chamber enlargement and impaired LV contractility. Although no significant difference in the absolute increase in LVEDD was observed, the absolute decrease in %FS and the absolute increases in LVESD and PW thickness were significantly greater in KO than in WT mice.

Changes in Heart Weights During Late Phase After MI

Among sham-operated animals, KO mice had larger heart weight-to-BW (HW/BW) ratios, which reflected basal myo-

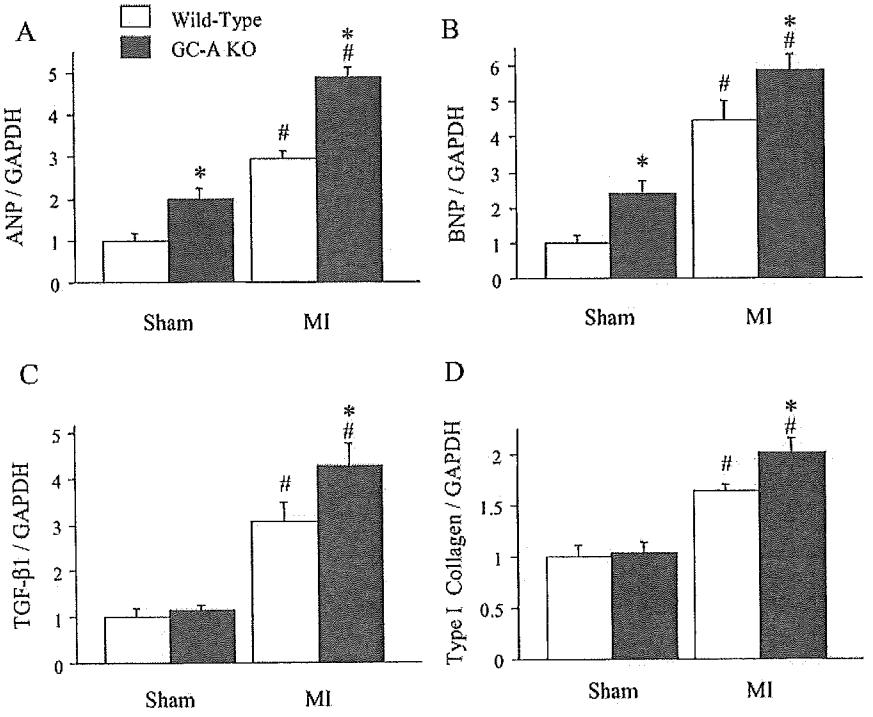

Figure 3. Relative levels of expression of ANP (A), BNP (B), TGF-β1 (C), and type I collagen (D) mRNA normalized to the corresponding GAPDH mRNA levels measured by quantitative RT-PCR in sham-operated and infarcted hearts 3 days after surgery. Mean mRNA levels in sham-operated WT hearts were assigned a value of 1.0. Values are means±SEM (n=7 to 10); *$P<0.05$ vs WT mice for each operation; #$P<0.05$ vs sham in each strain.

cardial hypertrophy (WT 5.44±0.14 mg/g versus KO 7.94±0.20 mg/g; $P<0.001$). Four weeks after MI, the HW/BW ratios were higher than in sham-operated mice, irrespective of genotype, but the effect was more pronounced in KO (Sham 7.94±0.20 mg/g versus MI 10.12±0.20 mg/g; 27% increase; $P<0.0001$) than WT (Sham 5.44±0.14 mg/g versus MI 6.29±0.14 mg/g; 16% increase; $P<0.005$) mice.

Myocardial Fibrosis During Late Phase After MI

As shown in Figure 4A, sections of ventricle from sham-operated KO mice showed significantly ($P<0.01$) more myocardial collagen accumulation than those from WT mice. Four weeks after MI, the collagen volume fraction in the noninfarcted septa was significantly increased in KO mice ($P<0.0001$) but not in WT mice ($P=0.6$). This marked difference in the degree of interstitial fibrosis in the noninfarcted septa from KO and WT mice can be seen in Figure 4B.

TABLE 2. Baseline, Week 4, and Absolute Changes From Baseline to Week 4 After MI in Echocardiographic Measurements

	WT (n=13)		GC-A KO (n=11)	
Parameters	Baseline	Week 4	Baseline	Week 4
Measurements				
LVEDD (mm)	4.55±0.08	5.76±0.08	5.11±0.10*	6.26±0.14*
LVESD (mm)	3.31±0.06	4.54±0.09	3.69±0.09*	5.28±0.12*
PWth (mm)	0.63±0.02	0.65±0.03	0.85±0.05*	1.02±0.04*
%FS (%)	27.4±0.3	21.5±1.0	27.5±0.6	15.6±0.9*
Absolute change from baseline to week 4 after MI				
Δ LVEDD (mm)	1.22±0.06		1.16±0.08	
Δ LVESD (mm)	1.24±0.09		1.59±0.09*	
Δ PWth (mm)	0.02±0.03		0.17±0.05*	
Δ %FS (%)	−5.9±1.1		−11.9±1.1*	

PWth indicates PW thickness.
Values are mean±SEM; *$P<0.05$ vs WT mice.

Effects of Genetic Disruption of AT1a Receptors in KO Mice

In an additional experiment, we induced MI in 8- to 10-week-old male DKO mice lacking GC-A and AT1a receptors. Although basal systolic blood pressures were significantly lower in DKO than KO mice (DKO 105.8±2.6 mm Hg; $P<0.0001$ versus KO mice), the high early mortality rate seen in the latter was not significantly improved in the former (Figure 5); and, as in KO mice, most of the deaths were attributable to acute heart failure (68.2%). Four weeks after MI, HW/BW ratios in DKO mice were 26% higher than in sham-operated animals (Sham 7.06±0.20 mg/g versus MI 8.88±0.42 mg/g; $P<0.001$), which is also similar to the response seen in KO mice. In contrast, there was no significant difference in the collagen volume fraction in the noninfarcted septa from infarcted and sham-operated DKO hearts (Figure 4A); indeed, the marked interstitial fibrosis seen in the noninfarcted septa from KO hearts was virtually absent in DKO hearts (Figure 4B).

Effects of Hydralazine Administration in KO Mice

To evaluate the involvement of blood pressure difference between WT and KO mice, we orally administered hydralazine to KO mice from 1 week before MI until 4 weeks after MI. Although systolic blood pressure was significantly reduced in hydralazine-treated KO mice (103.6±1.2 mm Hg; $P<0.0001$ versus nontreated KO mice), the high early mortality rate was not significantly improved (Figure 5), and histological analysis showed there to be no significant attenuation of the interstitial fibrosis in the noninfarcted septum 4 weeks after MI (Figure 4).

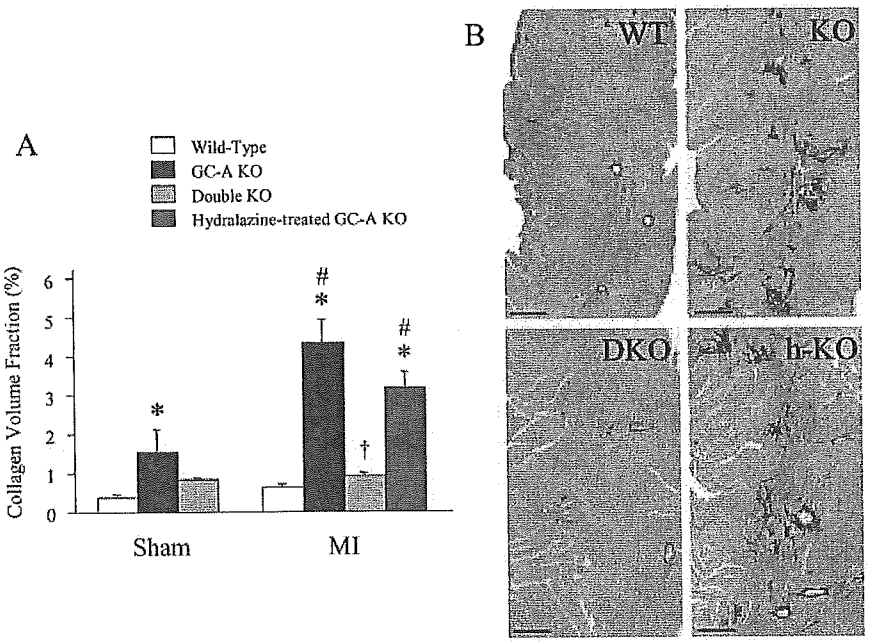

Figure 4. A. Evaluation of collagen volume in sham-operated hearts and noninfarcted regions of infarcted hearts from WT, GC-A KO, DKO, and hydralazine-treated GC-A KO mice 4 weeks after surgery. Values are means±SEM (n=6 to 9); *P<0.05 vs WT mice for each operation; #P<0.05 vs sham-operated KO mice; †P<0.0001 vs KO mice with MI. B, Representative van Gieson–stained sections showing noninfarcted regions in infarcted hearts from WT, GC-A KO (KO), DKO, and hydralazine-treated GC-A KO (h-KO) mice. Images show the interstitial collagen deposition (red staining) 4 weeks after induction of MI. Bars=200 μm.

Discussion

Although plasma ANP and BNP levels are known to be elevated early after MI,[11] their function in that context has been unclear. The present study shows that disrupting GC-A in mice results in a higher incidence of acute heart failure leading to increased early mortality and, later, in exaggerated LV dysfunction and remodeling. Thus, natriuretic peptides appear to exert beneficial effects during the early and late stages after MI.

During the 4-week study period, almost all deaths among both genotypes occurred within the first week after MI and were the result of heart failure or LV rupture. This survival pattern suggests that the rapid worsening of hemodynamics and mechanical stress after MI is, for the most part, compensated by the end of 1 week and stable for ≥3 weeks thereafter. In contrast to our previous study performed using an ischemia-reperfusion model,[13] infarct sizes were similar among the 2 genotypes, which is likely because permanent coronary occlusion changes the entire area at risk into infarction. This enabled us to compare the mortality rates and chronic LV remodeling resulting from similar insults in the 2 groups. Despite similar infarct sizes, the 1-week mortality rate was markedly higher in KO than WT mice. Postmortem findings indicate that the higher 1-week mortality rate in KO mice is attributable to a higher incidence of acute heart failure, which is consistent with the higher levels of cardiac expression of ANP and BNP mRNA observed in KO mice early after MI. Together, these results indicate that KO mice have a diminished capacity to compensate for acute heart failure after MI.

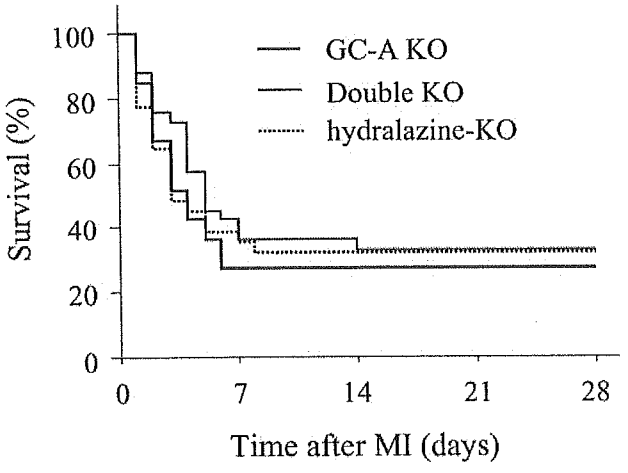

Figure 5. Kaplan–Meier analysis of survival after MI among GC-A KO (n=33), DKO mice (n=33), and hydralazine-treated GC-A KO (hydralazine-KO; n=31) mice. DKO mice and hydralazine-treated GC-A KO showed no significant improvement in 4-week survival over GC-A KO mice.

KO mice excreted less water and sodium than WT mice after MI, despite similar excretion during the early phase after the sham operation. Previous studies have shown that the infusion of 0.9% NaCl containing 4% albumin (isooncotic solution) results in impaired diuretic and natriuretic responses in GC-A KO mice, whereas the infusion of physiological saline (isotonic solution) leads to normal renal responses.[18] Because CHF could cause isooncotic volume expansion, the impaired renal response after MI in GC-A KO mice is consistent with the idea that GC-A plays an important role in diuresis and natriuresis under such pathological conditions as heart failure, although it is not essential under basal conditions.

Natriuretic peptides are known to act as negative regulators of renin-angiotensin-aldosterone system. Indeed, we showed previously that cardiac responsiveness to angiotensin II was significantly enhanced in the absence of GC-A,[16] and a previous study reported that natriuretic peptides reduced gene expression of aldosterone synthase in cultured neonatal rat cardiocytes.[19] In addition, there is clinical and experimental evidence that suppression of RAS activity reduces postinfarction mortality.[1,3,4] Therefore, we hypothesized that the higher mortality in KO mice was associated with greater activation

of RAS resulting from the lack of GC-A–mediated inhibition. To test that hypothesis, we compared postinfarction survival rates in GC-A KO and DKO mice, which lack GC-A and AT1a receptors. However, surprisingly, the 4-week survival rate for DKO mice was no better than that for KO mice, despite their significantly lower basal blood pressures (to a level similar to WT mice), and again most deaths were attributable to acute heart failure. Apparently, the protective role against heart failure played by GC-A early after MI is not mediated by reduction of blood pressure or inhibition of RAS.

GC-A attenuates chronic cardiac remodeling in a pressure-overload model (transverse aortic constriction)[20] and in a chronic hypoxia model.[21] The present study demonstrates that GC-A also attenuates cardiac hypertrophy and fibrosis and impaired LV contractility during the chronic phase after MI. Because previous studies have shown that inhibition of RAS diminishes LV remodeling after MI,[1,4] we were also interested in comparing LV remodeling in DKO and GC-A KO mice. Notably, the patterns of development of myocardial fibrosis and cardiac hypertrophy differed in the 2 genotypes (ie, the augmented fibrotic response was virtually abolished in DKO mice, although there was no attenuation of the enhanced hypertrophic response). Because previous reports have shown that natriuretic peptides exert a direct local antihypertrophic effect in vivo[20,22] and in vitro,[23] it is suggested that a direct action mediated via GC-A expressed on cardiac myocytes may be important after MI. We also evaluated the fibrotic response in hydralazine-treated GC-A KO mice, for which blood pressures were similar to those of DKO mice. However, hydralazine did not significantly affect the fibrotic response in KO mice, indicating the antifibrotic effect of GC-A is mediated mainly through inhibition of RAS, including aldosterone, not through reduction of blood pressure.

A recent clinical trial demonstrated that intravenous infusion of nesiritide (synthetic human BNP) improves the hemodynamic function and clinical status of patients with decompensated CHF.[10] Although patients with recent MIs were excluded from that trial, the present study suggests that infusion of BNP could also have beneficial effects in patients with heart failure early after MI. In addition, a study of 60 Japanese patients with anterior MI showed that infusion of carperitide (recombinant ANP) suppressed LV remodeling evaluated 1 month after MI better than nitroglycerin did.[24] Certainly, the lack of an oral form makes the use of natriuretic peptides somewhat impractical for long-term treatment; nevertheless, therapeutic strategies aimed at increasing levels of endogenous natriuretic peptides might be beneficial for patients after MI and deserve further investigation.

Functional deletion of the 5′-flanking region of the GC-A gene reduces transcriptional activity and is associated with essential hypertension and LV hypertrophy.[25] This means that individuals with congenital or acquired GC-A deficiencies would likely be at higher risk of death and exaggerated LV remodeling after MI. Perhaps genotyping the GC-A locus would be a useful approach to identifying these patients, thereby enabling early preventative measures to be taken.

Perspectives

Activation of GC-A by endogenous natriuretic peptides after MI prevents acute heart failure and attenuates chronic LV remodeling. Although these beneficial effects are mediated partly through inhibition of RAS activity, RAS-independent protective actions of GC-A are also suggested. The results of this study are suggestive of the potential for using exogenous ANP or BNP to improve short- and long-term outcomes among MI patients.

Acknowledgments

This work was supported by research grants from the Japanese Ministry of Education, Science, and Culture; the Japanese Ministry of Health and Welfare; the Japanese Society for the Promotion of Science Research for the Future program; and the KANAE Foundation for Life and Socio-Medical Science. GC-A KO mice were originally generated at the University of Texas, Southwestern Medical Center in Dallas and the Howard Hughes Medical Institute. We thank Kana Okamura and Komaki Okazaki for their excellent secretarial work and Mikako Inoue for her technical help.

References

1. Gruppo Italiano per lo Studio della Sopravvivenza nell'infarto Miocardico. GISSI-3: effects of lisinopril and transdermal glyceryl trinitrate singly and together on 6-week mortality and ventricular function after myocardial infarction. *Lancet.* 1994;343:1115–1122.
2. Dargie HJ. Effect of carvedilol on outcome after myocardial infarction in patients with left-ventricular dysfunction the CAPRICORN randomized trial. *Lancet.* 2001;357:1385–1390.
3. Pfeffer MA, McMurray JJV, Velazguez EJ, Rouleau JI, Kober L, Maggioni AP, Solomon SD, Swedberg K, Werf FV, White H, Leimberger JD, Henis M, Edwards S, Zelenkofske S, Sellers MA, Califf RM; Valsartan in Acute Myocardial Infarction Trial Investigators. Valsartan, captopril, or both in myocardial infarction complicated by heart failure, left ventricular dysfunction, or both. *N Engl J Med.* 2003;349:1893–1906.
4. Harada K, Sugaya T, Murakami K, Yazaki Y, Komuro I. Angiotensin II type 1A receptor knockout mice display less left ventricular remodeling and improved survival after myocardial infarction. *Circulation.* 1999;100:2093–2099.
5. Nakao K, Ogawa Y, Suga S, Imura H. Molecular biology and biochemistry of the natriuretic peptide system. II: Natriuretic peptide receptors. *J Hypertens.* 1992;10:1111–1114.
6. Yoshimura M, Yasue H, Okumura K, Ogawa H, Jougasaki M, Mukoyama M, Imura H. Different secretion patterns of atrial natriuretic peptide and brain natriuretic peptide in patients with congestive heart failure. *Circulation.* 1993;87:464–469.
7. Maisel AS, Krishnaswamy P, Nowak RM, McCord J, Hollander JE, Duc P, Omland T, Storrow AB, Abraham WT, Wu AH, Clopton P, Steg PG, Westheim A, Knudsen CW, Perez A, Kazanegra R, Herrmann HC, McCullough PA; Breathing Not Properly Multinational Study Investigators. Rapid measurement of B-type natriuretic peptide in the emergency diagnosis of heart failure. *N Engl J Med.* 2002;347:161–167.
8. Stanek B, Frey B, Hulsmann M, Berger R, Sturm B, Strametz-Juranek J, Bergler-Klein J, Moser P, Bojic A, Hartter E, Pacher R. Prognostic evaluation of neurohormonal plasma levels before and during beta-blocker therapy in advanced left ventricular dysfunction. *J Am Coll Cardiol.* 2001;38:436–442.
9. Troughton RW, Frampton CM, Tandle TG, Espiner EA, Nicholls MG, Richards AM. Treatment of heart failure guided by plasma aminoterminal brain natriuretic peptide (N-BNP) concentrations. *Lancet.* 2000;355:1126–1130.
10. Colucci WS, Elkayam U, Horton DP, Abraham WT, Bourge RC, Johnson AD, Wagoner LE, Givertz MM, Liang CS, Neibaur M, Haught WH, LeJemtel TH. Intravenous nesiritide, a natriuretic peptide, in the treatment of decompensated congestive heart failure. *N Engl J Med.* 2000;343:246–253.
11. Morita E, Yasue H, Yoshimura M, Ogawa H, Jougasaki M, Matsumura M, Mukoyama M, Nakao K. Increased plasma levels of brain natriuretic peptide in patients with acute myocardial infarction. *Circulation.* 1993;88:82–91.

12. Omland T, Aakvaag A, Bonarjee VV, Caidahl K, Lie RT, Nilson DW, Sundsfjord JA, Dickstein K. Plasma brain natriuretic peptides as an indicator of left ventricular systolic function and long-term survival after acute myocardial infarction. *Circulation.* 1996;93:1963–1969.
13. Izumi T, Saito Y, Kishimoto I, Harada M, Kuwahara K, Hamanaka I, Takahashi N, Kawakami R, Li Y, Takemura G, Fujiwara H, Garbers DL, Mochizuki S, Nakao K. Blockade of the natriuretic peptide receptor guanylyl cyclase-A inhibits NF-κB activation and alleviates myocardial ischemia/reperfusion injury. *J Clin Invest.* 2001;108:203–213.
14. Lopez MJ, Wong SKF, Kishimoto I, Dubois S, Mach V, Friesen J, Garbers DJ, Beuve A. Salt-resistant hypertension in mice lacking the guanylyl cyclase-A receptor for atrial natriuretic peptide. *Nature.* 1995; 378:65–68.
15. Pfeffer MA, Pfeffer JM, Fishbein MC, Fletcher PJ, Spadaro J, Kloner RA, Braunwald E. Myocardial infarct size and ventricular function in rats. *Circ Res.* 1979;44:503–512.
16. Li Y, Kishimoto I, Saito Y, Harada M, Kuwahara K, Izumi T, Takahashi N, Kawakami R, Tanimoto K, Nakagawa Y, Nakanishi M, Adachi Y, Garbers DL, Fukamizu A, Nakao K. Guanylyl cyclase-A inhibits angiotensin II type 1a receptor-mediated cardiac remodeling, an endogenous protective mechanism in the heart. *Circulation.* 2002;106:1722–1728.
17. Oliver PM, Fox JE, Kim R, Rockman HA, Kim HS, Reddick RL, Pandey KN, Milgram SL, Smithies O, Maeda N. Hypertension, cardiac hypertrophy, and sudden death in mice lacking natriuretic peptide receptor A. *Proc Natl Acad Sci U S A.* 1997;94:14730–14735.
18. Kishimoto I, Dubois SK, Garbers DL. The heart communicates with the kidney exclusively through the guanylyl cyclase-A receptor: acute handling of sodium and water in response to volume expansion. *Proc Natl Acad Sci U S A.* 1996;93:6215–6219.
19. Ito T, Yoshimura M, Nakamura S, Nakayama M, Shimasaki Y, Harada E, Mizuno Y, Yamamuro M, Harada M, Saito Y, Nakao K, Kurihara H, Yasue H, Ogawa H. Inhibitory effect of natriuretic peptides on aldosterone synthase gene expression in cultured neonatal rat cardiocytes. *Circulation.* 2003;107:807–810.
20. Knowles JW, Esposito G, Mao L, Hagaman JR, Fox JE, Smithies O, Rockman HA, Maeda N. Pressure-independent enhancement of cardiac hypertrophy in natriuretic peptide receptor A-deficient mice. *J Clin Invest.* 2001;107:975–984.
21. Klinger JR, Warburton RR, Pietras L, Oliver P, Fox J, Smithies O, Hill NS. Targeted disruption of the gene for natriuretic peptide receptor-A worsens hypoxia-induced cardiac hypertrophy. *Am J Physiol Heart Circ Physiol.* 2002;282:H58–H65.
22. Holtwick R, Eickels MV, Skryabin BV, Baba HA, Bubikat A, Begrow F, Schneider MD, Garbers DL, Kuhn M. Pressure-independent cardiac hypertrophy in mice with cardiomyocyte-restricted inactivation of the atrial natriuretic peptide receptor guanylyl cyclase-A. *J Clin Invest.* 2003;111: 1399–1407.
23. Horio T, Nishikimi T, Yoshihara F, Matsuo H, Takishita S, Kanagawa K. Inhibitory regulation of hypertrophy by endogenous atrial natriuretic peptide in cultured cardiac myocytes. *Hypertension.* 2000;35:19–24.
24. Hayashi M, Tsutamoto T, Wada A, Maeda A, Mabuchi N, Tsutsui T, Horie H, Ohnishi M, Kinoshita M. Intravenous atrial natriuretic peptide prevents left ventricular remodeling in patients with first anterior acute myocardial infarction. *J Am Coll Cardiol.* 2001;37:1820–1826.
25. Nakayama T, Soma M, Takahashi Y, Rehemudula D, Kanmatsuse K, Furuya K. Functional deletion mutation of the 5′-flanking region of type A human natriuretic peptide receptor gene and its association with essential hypertension and left ventricular hypertrophy in the Japanese. *Circ Res.* 2000;86:841–845.

Calcineurin–Nuclear Factor of Activated T Cells Pathway–Dependent Cardiac Remodeling in Mice Deficient in Guanylyl Cyclase A, a Receptor for Atrial and Brain Natriuretic Peptides

Takeshi Tokudome, MD, PhD; Takeshi Horio, MD, PhD; Ichiro Kishimoto, MD, PhD; Takeshi Soeki, MD, PhD; Kenji Mori, PhD; Yuhei Kawano, MD, PhD; Masakazu Kohno, MD, PhD; David L. Garbers, PhD; Kazuwa Nakao, MD, PhD; Kenji Kangawa, PhD

Background—Although disruption of guanylyl cyclase (GC) A, a natriuretic peptide receptor, induces cardiac hypertrophy and fibrosis, the molecular mechanism underlying these effects are not well understood. In this study, we examined the role of calcineurin, a calcium-dependent phosphatase, in cardiac remodeling in GCA-knockout (GCA-KO) mice.

Methods and Results—At 14 weeks of age, calcineurin activity, nuclear translocation of nuclear factor of activated T cells c3 (NFATc3), and modulatory calcineurin-interacting protein 1 (MCIP1) gene expressions were increased in the hearts of GCA-KO mice compared with wild-type (WT) mice. Blockade of calcineurin activation by FK506 (6 mg/kg body weight administered subcutaneously once a day from 10 to 14 weeks of age) significantly decreased the heart-to-body weight ratio, cardiomyocyte size, and collagen volume fraction in GCA-KO mice, whereas FK506 did not affect these parameters in WT mice. Overexpression of atrial and brain natriuretic peptides, collagen, and fibronectin mRNAs in GCA-KO mice was also attenuated by FK506. Electrophoretic mobility shift assays demonstrated that GATA4 DNA-binding activity was increased in GCA-KO mice, and this increase was inhibited by calcineurin blockade. In neonatal cultured cardiac myocytes, inhibition of GCA by HS142-1 (100 μg/mL) increased basal and phenylephrine (10^{-6} mol/L)-stimulated calcineurin activity, nuclear translocation of NFATc3, and MCIP1 mRNA expression. In contrast, activation of GCA by atrial natriuretic peptide (10^{-6} mol/L) inhibited phenylephrine (10^{-6} mol/L)-stimulated nuclear translocation of NFATc3.

Conclusions—These results suggest that activation of cardiac GCA by locally secreted natriuretic peptides protects the heart from excessive cardiac remodeling by inhibiting the calcineurin-NFAT pathway. (***Circulation.*** **2005;111:3095-3104.)**

Key Words: calcineurin ■ fibrosis ■ hypertrophy ■ natriuretic peptides ■ remodeling

Atrial natriuretic peptide (ANP) and brain natriuretic peptide (BNP) are cardiac hormones that act through guanylyl cyclase A (GCA) to lower blood pressure (BP), induce diuresis/natriuresis, and dilate blood vessels.[1,2] Cardiac synthesis and secretion of ANP and BNP are increased during cardiac hypertrophy associated with various cardiovascular diseases.[1] We and other groups have demonstrated the existence of natriuretic peptide receptors in cardiac cells.[3–5] Therefore, apart from acting as circulating hormones, ANP and BNP may have some functionality as autocrine and/or paracrine factors. Indeed, we have previously reported in an in vitro study that endogenous natriuretic peptides inhibit cardiac myocyte hypertrophy under basal and phenylephrine (PE)-stimulated conditions, probably via a cyclic GMP–dependent process.[6] Furthermore, we[7] and other groups[8] have reported that mice with disrupted GCA exhibit cardiac hypertrophy and interstitial fibrosis as well as hypertension. Cardiac hypertrophy in GCA-knockout (GCA-KO) mice is disproportionate to the increase in BP[9] and is resistant to antihypertensive medication.[10] We previously reported that overproduction of GCA in the cardiac myocytes of GCA-KO mice reduced cardiac myocyte size without altering BP.[11] In addition, mice with cardiomyocyte-restricted GCA disruption exhibited cardiac hypertrophy.[12] These findings suggest that GCA plays an in situ role in protecting the heart from abnormal remodeling independent of BP. However, the mo-

Received October 3, 2004; revision received January 23, 2005; accepted February 3, 2005.

From the Department of Biochemistry, Research Institute (T.T., I.K., T.S., K.M., K.K.) and Department of Medicine (T.H., Y.K.), National Cardiovascular Center, Suita, Osaka, Japan; the Second Department of Internal Medicine (M.K.), Kagawa University Faculty of Medicine, Kagawa, Japan; the Howard Hughes Medical Institute and Department of Pharmacology (D.L.G), University of Texas Southwestern Medical Center at Dallas; and the Department of Medicine and Clinical Science (K.N), Kyoto University Graduate School of Medicine, Kyoto, Japan.

Correspondence to Ichiro Kishimoto, MD, Department of Biochemistry, National Cardiovascular Center Research Institute, 5-7-1, Fujishirodai, Suita, Osaka 565-8565, Japan. E-mail kishimot@ri.ncvc.go.jp

Circulation **is available at http://www.circulationaha.org** **DOI: 10.1161/CIRCULATIONAHA.104.510594**

lecular mechanism underlying the inhibition of cardiac hypertrophy and fibrosis by GCA is not well understood.

A number of studies have attempted to elucidate the molecular mechanisms of the hypertrophic process in cardiac myocytes. Recently, Molkentin et al[13] and Vega et al[14] demonstrated the importance of calcineurin in the development of cardiac hypertrophy. Calcineurin (PP2B) is a calcium/calmodulin-activated serine-threonine phosphatase that is activated by sustained elevations in intracellular calcium.[15–17] Calcineurin dephosphorylates nuclear factor of activated T cells (NFAT).[18] The NFAT transcription factor is normally hyperphosphorylated and sequestered in the cytoplasm. However, on stimulation, NFAT is dephosphorylated by calcineurin and rapidly translocates to the nucleus.[18] In the nucleus, NFAT associates with GATA4, a zinc finger transcription factor, which directly regulates cardiac hypertrophy-related genes.[13,14] Calcineurin activity is suppressed by association with modulatory calcineurin-interacting protein 1 (MCIP1), which was cloned as the product of the Down syndrome critical region gene on chromosome 21.[14] MCIP1 is upregulated by calcineurin signaling and has been proposed to function in a negative-feedback loop to modulate calcineurin activity.[14] Two calcineurin inhibitors, cyclosporine A and FK506, have been shown to prevent cardiac hypertrophy and fibrosis in various models,[19–23] suggesting that calcineurin may play a pivotal role in cardiac remodeling. However, the physiological and pathophysiological regulation of the calcineurin-NFAT pathway is poorly understood. In this study, we have investigated the molecular mechanism of GCA-mediated inhibition of cardiac remodeling and have focused on the regulation of the calcineurin-NFAT pathway. Our results suggest that the cardiac natriuretic peptides-GCA system is an endogenous mechanism for monitoring cardiac hypertrophy by negatively regulating excessive activation of the calcineurin-NFAT pathway.

Methods

Animals and Treatment

All experimental procedures conformed to the guidelines for animal experimentation of the National Cardiovascular Center. GCA-KO mice were generated by methods described previously.[7] The genetic background of the original GCA-KO mice was a mixture of C57BL/6 and 129SVj. Genotypes were determined by using polymerase chain reaction. All comparisons were made among littermates. Male mice were examined at 14 weeks. Pharmacological treatment was begun when the animals reached 10 weeks of age. FK506, a calcineurin inhibitor (a gift from Fujisawa Industries Ltd), was administered subcutaneously at a dose of 6 mg/kg body weight once a day for 4 weeks. Vehicle alone was administered to control mice.

Measurement of BP and Heart Rate

Systolic BP (SBP) and heart rate (HR) were measured just before and after pharmacological treatment in conscious mice by the tail-cuff method (Softron Co Ltd).

Transthoracic Echocardiographic Study

Mice were anesthetized with intraperitoneal administration of ketamine (50 mg/kg) and xylazine (10 mg/kg), their chests were shaved, and 2-dimensional guided M-mode tracings of a cross section of the left ventricular minor axis at the tips of the papillary muscles were obtained for calculation with an echocardiographic system equipped with a 15-MHz phased-array transducer (Sonos-5500, Hewlett Packard).

Assay of Calcineurin Activity

Calcineurin activity was determined in lysates of whole ventricular tissues and cultured cardiac myocytes as previously described with some modifications.[24] For the phosphatase assay, RII peptide (Sigma) was phosphorylated by protein kinase A (Calbiochem) in the presence of [γ-^{32}P]ATP overnight at 30°C in the presence of 1 mol/L Tris-HCl (pH 7.5), 0.1 mol/L dithiothreitol, and 0.1 mol/L $MgCl_2$. Tissues and cells were homogenized in lysis buffer (50 mmol/L Tris-HCl [pH 7.5], 0.1 mmol/L EDTA, 0.1 mmol/L EGTA, 1 mmol/L dithiothreitol, 0.2% NP-40, and protease inhibitor cocktail). After the debris was removed by centrifugation, the supernatant was incubated with phosphorylated RII peptide for 30 minutes at 30°C. Okadaic acid (500 nmol/L) was added to the reactions to specifically suppress endogenous protein phosphatase PP1 and PP2A.[25] The amount of liberated ^{32}P was determined by the Cherenkov method.

Immunoprecipitation/Western Blot Analysis

Nuclear proteins of ventricles were extracted with NE-PER nuclear and cytoplasmic extraction reagents (Pierce) according to the manufacturer's instructions and were immunoprecipitated with anti-NFATc3 polyclonal antibody (Santa Cruz Biotechnology) in low-stringency buffer for 2 hours at 4°C and incubated with protein A beads (Roche) for 1 hour at 4°C. The immunoprecipitates were washed 4 times in phosphate-buffered saline and resuspended with 3× sodium dodecyl sulfate sample buffer. After the immunoprecipitate were heated to 95°C for 5 minutes, the samples were subjected to Western blot analysis. Western blot analyses were performed as described previously.[5] Samples were electrophoresed through a reducing sodium dodecyl sulfate–polyacrylamide gel and electroblotted onto a nitrocellulose membrane. The membrane was blocked with 5% nonfat dry milk and incubated with antibody for NFATc3. The expression levels of the proteins were detected with a Phototope-HRP Western Blot Detection System (Cell Signaling Technology). The band intensity was estimated with the use of NIH Image software.

Northern Blot Analysis

Total RNA (15 μg/lane) was extracted from whole ventricles with TRIzol (Invitrogen) reagent, denatured with formaldehyde and formamide, and electrophoresed on a 1% agarose gel containing formaldehyde. RNA in the gel was then transferred to a nylon membrane and fixed by UV irradiation. Hybridization and washing of the membrane were performed with cDNA probes for rat MCIP, murine ANP, rat BNP, rat α1 (type I) collagen, rat α1 (type III) collagen, rat fibronectin, and glyceraldehyde-3-phosphate dehydrogenase (GAPDH) genes and an oligonucleotide probe for 18S ribosomal RNA according to methods previously reported.[6] The band intensity was estimated with a radioimage analyzer (BAS-5000, Fuji Film).

In Situ Hybridization

A digoxigenin-labeled cRNA probe specifically hybridized to the murine MCIP1 mRNA was made by reverse transcription–polymerase chain reaction and in vitro transcription. Deparaffinized sections were permeabilized and digested with proteinase K (Gibco). After postfixation, acetylated sections were incubated with the cRNA probe at 55°C overnight. After being washed with 0.1× standard saline citrate, the probe was detected with a streptavidin–horseradish peroxidase conjugate and tyramide-based amplification with a diaminobenzidine substrate (Dako).

Histological Examination

The ventricles were fixed with 4% paraformaldehyde in phosphate-buffered saline and prepared for routine histological examination. Paraffin sections (2 μm) were stained with hematoxylin and eosin for measurement of myocyte size and diameter and with Sirius red

F3BA for determination of collagen volume fraction. For measurement of cardiomyocyte cross-sectional area and width, a total of 30 myocytes sectioned transversely at the level of the nucleus were randomly chosen from each section at ×400 magnification and traced. To measure collagen volume fraction, 16 fields of left ventricle wall per section were scanned and digitized with an Optima 6.5 digital image analyzer (Media Cybernetics) at ×200 magnification. The interstitial collagen volume fraction was measured while omitting fibrosis of the perivascular, epicardial, and endocardial areas from the study. The collagen volume fraction was obtained by calculating the mean ratio of connective tissue to the total tissue area of all measurements of the section.

Electrophoretic Mobility Shift Assay

Electrophoretic mobility shift assays (EMSAs) were performed as described previously.[5] Nuclear proteins were extracted with NE-PER nuclear and cytoplasmic extraction reagents (Pierce) according to the manufacturer's instructions, and EMSA was performed with a LightShift chemiluminescent EMSA kit (Pierce). For EMSA, the binding reactions were performed for 20 minutes in 10 mmol/L Tris-HCl (pH 7.5), 50 mmol/L KCl, 5 mmol/L $MgCl_2$, 1 mmol/L dithiothreitol, 50 ng/μL poly(dI-dC)(dI-dC), 0.05% NP-40, 2.5% glycerol, biotin 3′-end-labeled double-stranded oligonucleotide, and nuclear protein extract. Samples were electrophoresed on a native polyacrylamide gel and then transferred to a nylon membrane. The biotin end-labeled DNA was detected by chemiluminescence. The nucleotide sequence of the sense strand of the double-stranded GATA oligonucleotide was 5′-CAC TTG ATA ACA GAA AGT GAT AAC TCT-3′. Supershift experiments were performed by incubating the nuclear extracts with 2 μg GATA4 polyclonal antibody (Santa Cruz Biotechnology).

Cell Culture

Primary cultures of neonatal ventricular myocytes were prepared as described previously.[6] In brief, apical halves of cardiac ventricles from 1- to 2-day-old Wistar rats were separated, minced, and dispersed with 0.1% collagenase type II (Worthington). To segregate myocytes from nonmyocytes, a discontinuous gradient of Percoll (Sigma) was prepared. After centrifugation, the upper layer consisted of a mixed population of nonmyocyte cell types, and the lower layer consisted almost exclusively of cardiac myocytes. After the myocytes were incubated twice on uncoated 10-cm culture dishes for 30 minutes to remove any remaining nonmyocytes, the nonattached viable cells were plated on gelatin-coated glass slides or culture dishes and then cultured in Dulbecco's modified Eagle's medium (DMEM, Gibco BRL) supplemented with 10% fetal calf serum (Gibco BRL). After a 24-hour incubation in DMEM with fetal calf serum, the culture medium was changed to serum-free DMEM, and all experiments were performed 24 hours later. This purification procedure has well been established,[26,27] and in fact, immunostaining with anti-rat sarcomeric antibody revealed that >99% of the cells obtained by this method were cardiomyocytes.[27]

Immunocytochemistry

Cardiac myocytes were grown on glass slides. The cells were fixed with 4% paraformaldehyde in phosphate-buffered saline for 15 minutes at room temperature. Immunocytochemical staining for NFATc3 and GATA4 was performed with the indirect immunofluorescence method. Cells were incubated with anti-NFATc3 polyclonal antibody (Santa Cruz Biotechnology) and anti-GATA4 polyclonal antibody (Santa Cruz Biotechnology) at dilutions of 1:50 and 1:200, respectively. The NFATc3 and GATA4 signals were detected with anti-rabbit fluorescein isothiocyanate–conjugated secondary antibody and an anti-goat tetramethylrhodamine B isothiocyanate–conjugated secondary antibody, respectively. A fluorescence microscope was used to visualize the cells at ×1000 magnification.

Statistical Analysis

All values are shown as mean±SEM. Statistical significance between the 2 groups was determined with an unpaired t test. For multiple comparisons, the data were subjected to 1-way ANOVA followed by the Bonferroni/Dunn test. Probability values of <0.05 were considered statistically significant.

Results

Calcineurin-NFAT Pathway Is Upregulated in GCA-KO Mice

At 14 weeks of age, there was no significant difference in HR between the genotypes (WT, 633.3±18.0 versus GCA-KO, 608.0±15.7 bpm; n=4 per group); however, moderate increases in SBP were observed in the GCA-KO mice (WT, 105.5±3.2 versus GCA-KO, 130.6±2.1 mm Hg [$P<0.05$], n=4 per group). As shown in Figure 1A, disruption of the *GCA* gene induced a significant increase in the heart-to-body weight ratio (WT, 3.92±0.05 versus GCA-KO, 5.99±0.21 [$P<0.05$]).

To determine whether deletion of *GCA* changed calcineurin activity, we performed calcineurin enzymatic assays. As shown in Figure 1B, a significant increase in calcineurin activity was observed in GCA-KO mice (WT, 168.8±12.0 versus GCA-KO, 252.6±5.6 cpm/μg protein [$P<0.05$]).

It has been shown that the NFATc3 transcription factor is a direct downstream effector of calcineurin in the heart and that NFATc3 translocates to the nucleus after calcineurin-mediated dephosphorylation.[28] Therefore, we examined whether NFATc3 translocation to the nucleus was increased in the hearts of GCA-KO mice. As shown in Figure 1C, the amount of NFATc3 protein in nuclear extracts was significantly higher in GCA-KO mice compared with their WT littermates (1.5-fold, $P<0.05$).

MCIP1 is upregulated by calcineurin signaling and has been proposed to function in a negative-feedback loop to modulate calcineurin activity.[14] *MCIP1* gene expression was significantly increased in the hearts of GCA-KO mice compared with WT hearts (3.5-fold, $P<0.05$; Figure 1D). Furthermore, we used in situ hybridization to investigate the cell types that expressed the *MCIP1* gene. As shown in Figure 1E, *MCIP1* gene expression was observed primarily in cardiac myocytes. Taken together, these results suggest that calcineurin is activated in cardiac myocytes of GCA-KO mice.

FK506 Suppresses Activation of Calcineurin in GCA-KO Mice Without Affecting Body Weight, SBP, or HR

Because the calcineurin-NFAT pathway was activated in GCA-KO mice, we next examined whether inhibition of calcineurin activity by FK506 could prevent cardiac hypertrophy and fibrosis in GCA-KO mice. Elevation of calcineurin activity in GCA-KO mice was suppressed completely by FK506 administration (6 mg/kg body weight administered subcutaneously once a day from 10 to 14 weeks of age, Figure 2A). Calcineurin activity in the WT mice was mildly but significantly suppressed. FK506 treatment had no effect on physiological increases in body weight, SBP, and HR in both WT and GCA-KO mice (Table 1). No remarkable side effects of FK506 treatment were seen in mice with either genotype, and all mice survived throughout the treatment protocol.

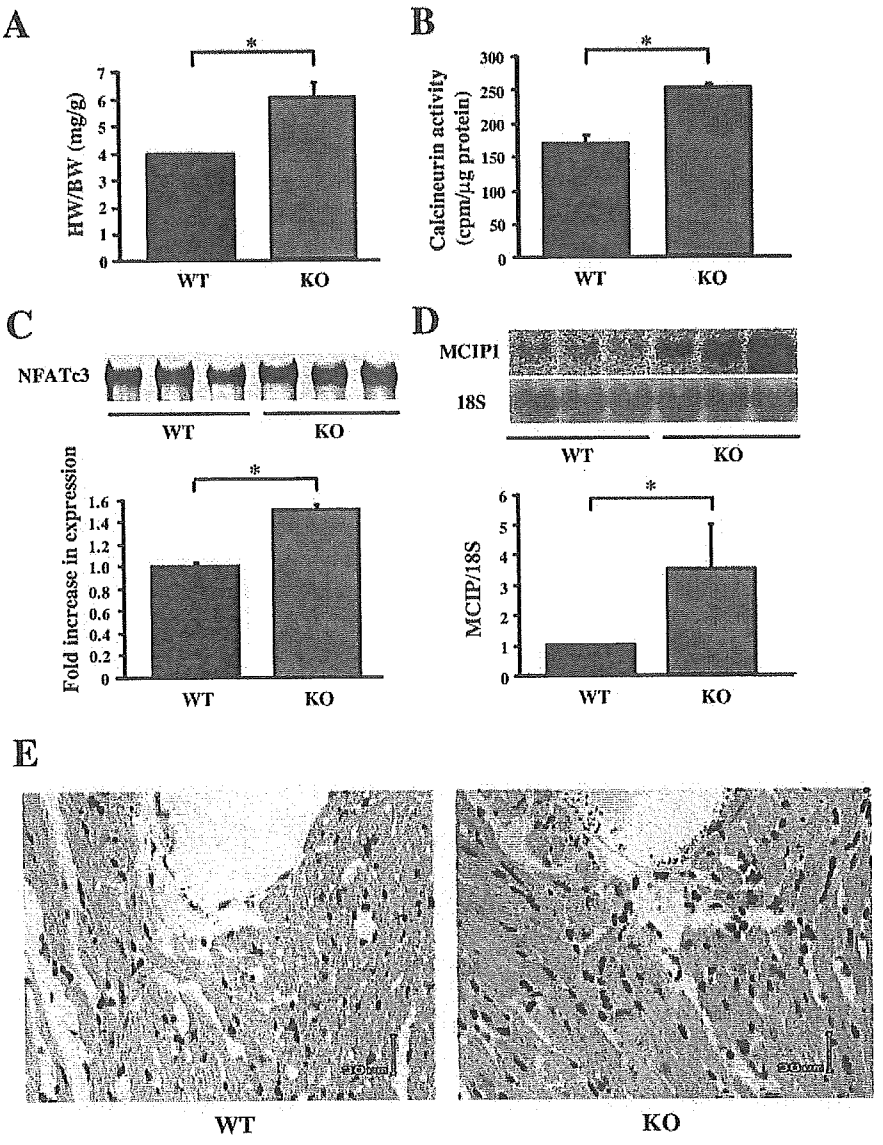

Figure 1. GCA disruption induces cardiac hypertrophy, calcineurin activation, nuclear translocation of NFATc3, and *MCIP1* gene expression in heart. A, Heart-to-body weight ratio (HW/BW) of animals. B, Calcineurin activity in hearts of animals. C, Immunoprecipitation and Western blot analysis of NFATc3. Nuclear protein extracts from whole ventricles were used as samples. D, Northern blot analysis of MCIP1 mRNA expression in hearts. Probe for 18S ribosomal RNA was used as loading control. E, Representative image of in situ hybridization of MCIP1 in hearts. Positive staining is brick red. Data are expressed as mean±SEM of n=3 or 4 animals per group. *$P<0.05$. Abbreviations are as defined in text.

FK506 Attenuates Cardiac Hypertrophy in GCA-KO Mice

As shown in Figure 2B, treatment with FK506 partially, but significantly attenuated the increase in the heart-to-body weight ratio in GCA-KO mice (GCA-KO+vehicle, 6.07±0.18 versus GCA-KO+FK506, 4.59±0.17 [$P<0.05$]). In contrast, FK506 treatment did not influence the heart-to-body weight ratio in WT mice (WT+vehicle, 3.80±0.11 versus WT+FK506, 3.62±0.13 [NS]).

As shown in Table 2, echocardiographic analysis demonstrated an increase in the thickness of the interventricular septum (IVSth) and left ventricle posterior wall (LVPWth) and an increase in the left ventricle diastolic dimension (LVDd) in GCA-KO mice. Fractional shortening did not differ significantly between WT and GCA-KO mice. Treatment with FK506 partially but significantly attenuated the increases in IVSth, LVPWth, and LVDd in GCA-KO mice but did not affect fractional shortening. In WT mice, FK506 did not change cardiac function or morphology. Representative images of M-mode echocardiograms are shown in Figure 2C.

Histological Analysis of FK506-Treated Mice

We next examined myocyte size and interstitial fibrosis in the left ventricle. In hematoxylin and eosin–stained sections, we observed an increase in cross-sectional myocyte area and width in the GCA-KO mice compared with WT mice; this increase was partially but significantly prevented by treatment with FK506 (Figure 3A-C). In contrast, FK506 did not affect myocyte area and width in WT mice.

To determine the degree of fibrosis, we performed Sirius red staining. Left ventricular interstitial fibrosis was 7-fold higher in GCA-KO mice than in WT mice. Excessive interstitial fibrosis in GCA-KO mice was also prevented by FK506 treatment (Figure 4A, 4B), whereas FK506 did not affect interstitial fibrosis in WT mice.

Calcineurin Activation Is Involved in Cardiac Gene Expression in GCA-KO Mice

ANP gene expression is increased by a variety of hypertrophic stimuli,[29] and both the expression and secretion of BNP are elevated in patients with cardiac hypertrophy.[30] As shown in Figure 5, ANP and BNP mRNA levels in the ventricle were